### **CHAPTER 36**

## Empirical Prediction of Wave Spectrum for Wind-Generated Gravity Waves

In the energy-containing range, an empirical frequency spectrum representing a general sea state was derived,

$$\frac{n_{o}^{3}\phi(n)}{u_{*}C_{o}} = A_{1} r \left(\frac{n}{n_{o}}\right)^{-r} \exp\left[-\frac{r}{r-1}\left(\frac{n}{n_{o}}\right)^{-r+1}\right].$$

Experimental data were used to verify this empirical frequency spectrum. The value of A was approximated to be 0.044 and the value of r is related to  $n_{u_{\star}}/g$  by

$$r = 9.1 \left(\frac{n_{o}u_{\star}}{g}\right)$$
 .

2

In the equilibrium range, the saturated frequency spectrum was approximated by

$$\frac{n_{o}^{3} \phi(n)}{u_{*}C_{o}} = 0.08 \left(\frac{n_{o}u_{*}}{g}\right)^{-1/4} \left(\frac{n_{o}}{n_{o}}\right)^{-5}$$

Experimental data were used to test whether the Phillips spectrum,  $\phi(n) = \beta g^2 n^{-5}$  would serve as a better approximation of the wave spectrum than the Toba spectrum,  $\phi(n) = \alpha u_{\star} g n^{-4}$ . Measurements of both the wave slope spectrum and the mean square wave slope favor the Phillips spectrum.

### Introduction

Wind-Generated gravity wave has been of great interest to researchers and engineers in the field of coastal engineering because it is one of the important considerations in the engineering studies and designs for ship navigation, coastal and off-shore structures, shore protection, oil pollution control, and wave energy conversion. An accurate prediction of the wave height, wave frequency, and wave spectrum is critical to the success of these engineering studies and designs.

Based on dimensional reasoning, Phillips (20) hypothesized that in the equilibrium range, the wave frequency spectrum of wind-generated gravity waves,  $\phi(n)$  is saturated and can be approximated by

\*ASCE member; President, United Industries Corp., 12835 Bell-Red Rd. #120, Bellevue, WA., U.S.A. 98005

$$\phi(n) = \beta g^2 n^{-5} \quad \text{for } n_0 << n << n_\gamma$$
 (1)

where g is the gravitational acceleration, n is the angular wave frequency, n is the wave frequency of the dominant wave, n is defined as  $(4g^{3}/\gamma)^{\frac{1}{2}}$ ,  $\gamma$  is the surface tension per unit density and  $\beta$  is a nondimensional numerical coefficient. To approximate the frequency spectrum in both the equilibrium range and the energy-containing range for fully developed wind waves in the open ocean, Pierson and Moskowitz (23) proposed the PM continuous frequency spectrum

$$\phi(n) = \beta g^2 n^{-5} \exp \left[-\frac{5}{4} \left(\frac{n}{n_o}\right)^{-4}\right]$$
 (2)

For a growing sea that the wind wave field has not yet reached the fully-developed stage, Hasselmann, et al, (6) proposed the JONSWAP continuous frequency spectrum

$$\phi(n) = \beta g^2 n^{-5} \exp \left[-\frac{5}{4} \left(\frac{n}{n_0}\right)^{-4}\right] \delta^{\Gamma}$$
(3)

Equation (3) was derived by multiplying the peak-enhancement function,  $\delta^{\Gamma}$ , to the PM spectrum expressed in Equation (2). Here  $\delta$  is the ratio of the spectral maximum to the spectral maximum derived from the PM spectrum,  $\Gamma$  is defined by  $\Gamma = \exp\left[-(n - n_0)^2/2\sigma_0^2\right]$ , and  $\sigma = \sigma_a$  for  $n \leq n_0$  and  $\sigma = \sigma_b$  for  $n \geq n_0$ .

Huang, et al. (8) proposed the unified two-parameter WALLOPS frequency spectrum to approximate the frequency spectrum in the energycontaining range for a general sea state

$$\phi(n) = \frac{\beta g^2}{n^m n_0^{5-m}} \exp\left[-\frac{m}{4} \left(\frac{n_0}{n}\right)^4\right]$$
(4)

When the value of m is equal to 5, Equation (4) is identical to the Pierson-Moskowitz spectrum.

Based on the three-second power law (Toba, 29a) and the concept of the similarity wave spectrum, Toba (29) proposed that in the equilibrium range,

$$\phi(n) = \alpha g u_{\star} n^{-4} \text{ for } n_{o} \leq n \leq n_{\gamma}$$

$$\phi(n_{o}) = \alpha_{o} g u_{\star} n_{o}^{-4}$$
(5a)

where  $u_{\star}$  is the frictional velocity of the wind, and  $\alpha$  and  $\alpha_{\circ}$  are non-dimensional numerical coefficients. A theoretical support for the  $n^{-4}$  equilibrium range was provided by Zakharov and Filonenko (32).

In analogy to the JONSWAP Spectrum, Donelan, et. al (4a) proposed a continuous wave spectrum which yields to the  $n^{-4}$  spectrum in the equilibrium range,

$$\phi(n) = \alpha_{d} g^{2} n^{-4} n_{o}^{-1} \exp\left[-\left(\frac{n}{o}\right)^{4}\right] \delta^{\Gamma}$$
(6)

where  $\alpha_{d}$  is a non-dimensional numerical coefficient. In a recent paper, Battjes, et. al (la) reanalyzed the JONSWAP data and concluded that the  $n^{-4}$  spectrum may fit the data as well as or even better than the  $n^{-5}$  spectrum.

For the present study, the wave spectrum is examined by using similarity analysis. An empirical equation was provided to approximate the wave spectrum in the energy-containing range. The wave spectrum behavior in the equilibrium range was analyzed and the slope measurements were used to determine which of the  $n^{-5}$  or  $n^{-4}$  spectrum is preferrable.

Similarity Wave Spectrum

By definition, the integration of the wave frequency spectrum,  $\phi(n)$ , over the whole frequency range between zero and  $\infty$  should be equal to  $n^2$ , i.e.,

$$\int_{0}^{\infty} \phi(n) \, dn = \overline{\eta^2}. \tag{7}$$

where  $\eta^2$  is the mean square of the vertical displacement from the mean water surface. Rewriting Equation (7) in a non-dimensional form

$$\int_{0}^{n} \frac{a^{\phi(n)}}{n^{2}} d\left(\frac{n}{n_{0}}\right) = 1$$
(8)

would provide an integral constraint on the function of  $\phi(n) n_0/n^2$ . Mitsuyasu (14) presented similarity frequency spectra by plotting  $\phi(n) n_0/n^2$  vs.  $n/n_0$  and showed that his laboratory data had different shape of similarity spectrum from his Hakata Bay data.

Equation (7) may be rewritten in another non-dimensional form

$$\int_{o}^{\infty} \frac{\phi(n)}{\phi(n_{o})} d\left(\frac{n}{n_{o}}\right) = \frac{\overline{\eta^{2}}}{n_{o}\phi(n_{o})}$$
(9)

As shown by Burling (1) and Mitsuyasu (14), the nondimensional parameter  $n^2/n_o \phi(n_o)$  can be approximated by a numerical constant, and, thus, plots of  $\phi(n)/\phi(n_o)$  vs.  $n/n_o$  would present another form of similarity frequency spectrum. Donelan, et. al (1985) presented both their laboratory and field data by plotting  $\phi(n)/\phi(n_o)$  vs.  $n/n_o$ , but the data cannot be collapsed into a single similarity shape. These two forms of similarity frequency spectrum presented above have the scaling factors, including the wave characteristics, such as  $\phi$  (n<sub>o</sub>), n<sub>o</sub>, and n<sup>2</sup>, while the wind speed, which is responsible for generating wind waves, is not explicitly included. From the point of view of predicting wave spectrum, these similarity spectrum forms may not be readily applicable. It is therefore the intention of this paper to obtain a similarity frequency spectrum that will be readily applicable in predicting wave spectrum.

In a recent paper to analyze the wind wave momentum equation  

$$\rho_{w}g \frac{d}{dt} \left(\frac{n}{C_{o}}\right) = \tau_{w}$$
(10)

Lin (11) proposed a closure approximation for the wind-wave momentum:

The wind-wave momentum per unit area per unit weight of water,  $n^2/C_0$ , is characterized by the wind frictional velocity  $u_*$ , and the dominant wave frequency  $n_0$ .

Here,  $\tau$  is the effective wind wave drag and  $\rho$  is the density of the water. By virtue of dimensional reasoning, he derived an empirical equation

$$\frac{\eta^2}{c_o} = A_1 \frac{u_*}{n_o^2}$$
(11)

where  $A_1$  is a nondimensional coefficient,  $C_0$  is the phase speed of the dominant wave,  $u_*$  is the frictional velocity of the wind defined as  $u_* = \sqrt{C_d} U_{10}$ ,  $C_d$  is the drag coefficient,  $U_{10}$  in m/sec is the wind speed at 10m above the water surface. For calculation of  $C_d$ , the empirical equations by Wu (30) were used,

$$C_d = 0.0026 \text{ for } U_{10} > 15 \text{ m/sec}$$
  
 $C_d = 0.0005 \sqrt{U_{10}} \text{ for } 1 < U_{10} < 15 \text{ m/sec.}$  (12)

Because of the importance of Equation (11) in supporting the present paper, experimental data used to verify Equation (11) are reproduced in Figure 1. These experimental data were obtained under a wide range of wind and wave conditions and in different seas around the world. The nondimensional coefficient  $A_1$  was determined to be 0.044 for wind waves in deep waters. It is expected that the numerical value of  $A_1$  could vary with the water depth and the current, and that it would depend on whether the wind wave field is in the growing or decaying stage. Equation (11) with  $A_1 = 0.044$  may be converted to

$$\varepsilon = 1.8 \times 10^{-4} \sqrt{C_d} v^{-3}$$
 (11a)

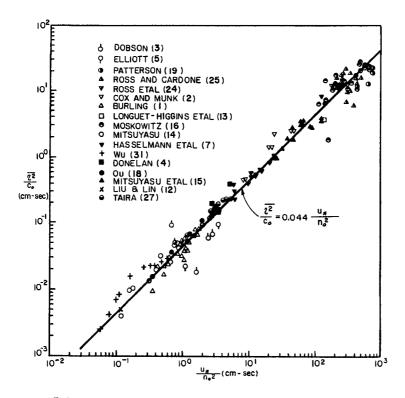


FIGURE I Wind - Wave Momentum Per Unit Area Per Unit Weight, 22/Co Vs u\*/ no<sup>2</sup>

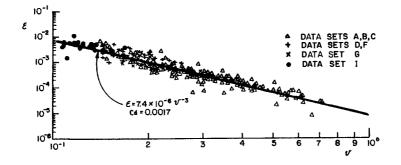


FIGURE 2 Variation of  $\mathcal{E}$  With v for Wind Waves.Data Available From Hasselmann, Etal (7) and Van Müller (17)

where  $\varepsilon = g^2 n^2/U_{10}^4$  and  $v = n_0 U_{10}/(2 \pi g)$ . In Figure 2, data available from Hasselmann, et al. (7) and Von Müller (17) are replotted. A solid line representing Equation (11a) with  $C_d = 0.0017$  for  $U_{10} = 12$  m/sec fit the data very well.

Using Equation (11), Equation (7) is rewritten as

$$\int_{0}^{\infty} \frac{n_{o}^{3}\phi(n)}{u_{*}c_{o}} d\left(\frac{n}{n_{o}}\right) = \frac{n^{2}n_{o}^{2}}{u_{*}c_{o}} = A_{1}$$
(13)

For wind waves in deep waters, the scaling factor of the frequency spectrum expressed in Equation (13) becomes  $u_{x}g/n_{o}^{4}$  which is consistent with that used by Toba (29).

In Figure 3, we plot  $n_o^3 \phi(n)/u_*C_o$  vs.  $n/n_o$  for wind wave data obtained in the laboratory wind-wave tanks by Mitsuyasu (14), by Toba (29), by Ou (18), and by Liu and Lin (12), and in the field by Burling (1) and Mitsuyasu (14). In Figure 4, several spectral measurements of the fully developed wind waves in open ocean conducted by Pierson (22), by Longuet-Higgins, et al. (13), by Ross and Cardone (25), and by Mitsuyasu, et al (15) are also presented in non-dimensional form as  $n_o^3 \phi(n)/u_*C_o$  vs.  $n/n_o$ .

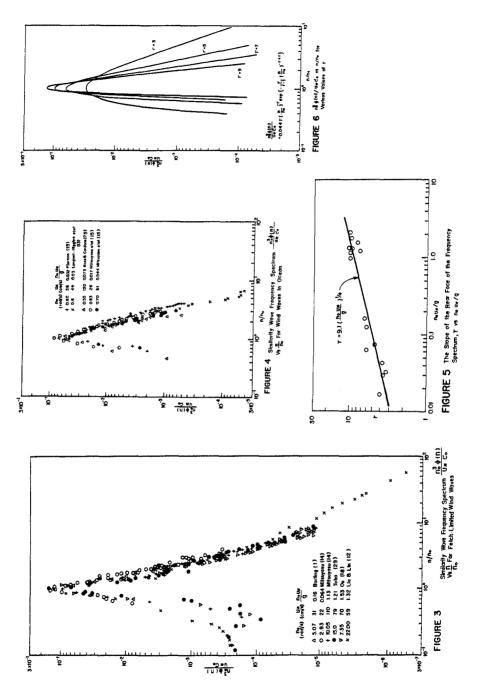
Energy-Containing Range

The energy-containing range may be defined as the frequency range in which the energy contained would represent the majority, say 95 percent, of the total wave energy. As shown in Figures 3 and 4, the slope of the rear face of the wave spectrum in the energy containing range, expressed as r in the power law:  $\phi(n) \sim n^{-r}$ , has a value as high as 10 for the laboratory data and it decreases as  $n_{0}u_{*}/g$ decreases. To obtain the variation of the r values with  $n_{0}u_{*}/g$ , the experimental data plotted in Figures 3 and 4 together with additional spectral data available from Burling (1) and Mitsuyas (14) were used. The data points shown in Figure 5 may be fitted approximately by a power law,

r = 9.1 
$$\left(\frac{n}{o} \frac{u_{\star}}{g}\right)^{1/4}$$
 for 0.017  $< \frac{n}{g} \frac{u_{\star}}{g} < 2.1$  (14)

The decrease of the rear face slope of the spectrum with the sea state may be attributed to the enhancement of the wave breaking process as the value of  $n_{o}u_{*}/g$  decreases.

To reflect the change of the spectral shape with the sea state, an empirical wave spectrum was derived as



$$\frac{n_{o}^{3}\phi(n)}{u_{\star}C_{o}} = A_{1} r(\frac{n}{n_{o}})^{-r} \exp\left[-\frac{r}{r-1} (\frac{n}{n_{o}})^{-r+1}\right]$$
(15)

Equation (15) can readily be integrated to satisfy Equation (13), and it also satisfies the condition that the spectrum peaks at n = n. The Pierson-Moskowitz spectrum is a special case of Equation (15) when r = 5. Another important feature of Equation (15) is that when the value of r increases with  $n_0 u_x/g$  according to Equation (14), the spectral peak increases. This feature is apparently consistent with the experimental data presented in Figures 3 and 4.

To illustrate the variation of the spectral shape with r, Equation (15) is presented in Figure 6 with  $A_1 = 0.044$ . Also we plot  $\phi(n)/\phi(n_0)$  vs  $n/n_0$  in Figure 7 as

$$\frac{\phi(n)}{\phi(n_0)} = (\frac{n}{n_0})^{-r} \exp\{-\frac{r}{r-1}[(\frac{n}{n_0})^{-r+1} - 1]\}.$$
(16)

The normalization of  $\phi(n)$  with respect to  $\phi(n)$  further accentuates the sharpening of the spectral shape when the value of r increases. In Figure 8, the analytical solutions expressed in Equation (15) for r = 10, 5 and 4 are presented for comparison with the experimental data obtained in the laboratory and in the field. The comparison is fairly well.

# Equilibrium Range

In the equilibrium range, the wave frequency spectrum, according to Phillip's concept, is saturated and governed by the gravitational acceleration. By fitting the experimental data presented in Figures 3 and 4 with the  $n^{-5}$  spectrum, one may find out that the value of ß in Equation (1) is not a universal constant. On the other hand, one may also estimate the value of  $\alpha$  as expressed in Equation (5) by fitting the experimental data with the  $n^{-4}$  spectrum. In Figure 9, the values of  $\beta(n_{o}u_{\star}/g)^{-1}$  and  $\alpha$  are plotted against  $n_{o}u_{\star}/g$ . Two solid lines are drawn to approximate the experimental data as

$$\beta = 0.08 \left(\frac{n_{o} u_{\star}}{g}\right)^{3/4}$$
(17)  
$$\alpha = 0.027 \left(\frac{n_{o} u_{\star}}{g}\right)^{-1/3}$$
(18)

Since the spectral measurements of wave variances could not accurately settle the difference between  $n^{-4}$  and  $n^{-5}$  in the equilibrium range, research effort was directed to analyzing the spectral

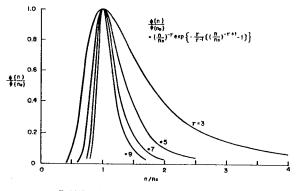
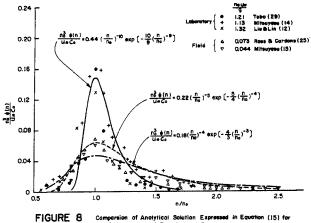
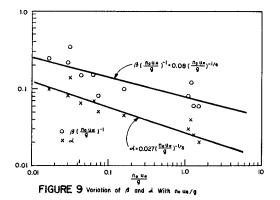


FIGURE 7 +(n1/+ (ne) vs n/ne for Various Values of r



Comparison of Analytical Solution Expressed in Equation (15) for  $\tau\approx 10,5,$  and 4, and Experimental Data



measurements of wave slopes. Using the dispersion relation  $n^2 = gk$  for gravity waves and  $\phi(n)dn = \chi(k)kdk$ , the wave-number spectrum  $\chi(k)$  corresponding to Equations (1) and (5) are derived respectively as follows:

a) Phillips spectrum  

$$\chi(k) = \frac{3}{2}k^{-4}$$
(19)

b) Toba spectrum

Ь)

$$\chi(\mathbf{k}) = \frac{\alpha}{2} u_{\mathbf{k}} g^{-1/2} \mathbf{k}^{-7/2} . \qquad (20)$$

Hence, the wave slope frequency spectrum  $\phi$  (n) in correspondence to Equations (19) and (20) are derived below:

a) Phillips spectrum  

$$\phi_{s}(n) = \beta n^{-1} \qquad (21)$$

Toba spectrum  

$$\phi_{s}(n) = \alpha \frac{u_{\star}}{g}$$
. (22)

Equation (22) suggests that, in the equilibrium range, the Toba spectrum would have a constant value, but this result is not supported by the limited data of wave slope spectra measured by Cox (2a) and by Long and Huang (12a).

Further testing may be made by comparing the mean square wave slope measurements and the analytical results based on Equations (19) and (20). According to Phillips (21) the mean square wave slope  $s^{\frac{2}{3}}$  of wind waves may be approximated by

$$\bar{s}^{2} = \int_{k_{0}}^{k_{v}} k^{2} \chi(k) k dk$$
(23)

Here  $k_{y}$  is the cut-off wave number, representing highest wave number of the gravity wave that could be excited by the wind. Hence, the mean square wave slope may be approximated by

$$\overline{s^2} = \frac{\beta}{2} \ln \frac{k_v}{k_o}$$
(24)

if Equations (19) and (23) are used, or by

$$\overline{s^2} = \alpha \frac{n_o u_{\star}}{g} \left( \sqrt{\frac{k_v}{k_o}} \right)$$
(25)

if Equations (20) and (23) are used.

Cox and Munk (2) conducted wave slope measurements of the sea surface covered with an artificial slick, and thus, the wave slope measurements were contributed from the gravity waves but not from the capillary waves. Since the measurements showed that wave components shorter than 30 cm were almost entirely absent (Phillips, (21)) k may be approximated by 2  $\pi/30$  cm<sup>-1</sup>. Longuet-Higgins, et al. (13) measured the wave slopes of wind waves in the open ocean. Since their measurements were filtered at 4 rad/sec, the cut-off wave number may be estimated using the dispersion relation as k = 4<sup>-</sup>/g. In Figure 10, both sets of wave slope measurements are presented and compared with Equation (24) having ß approximated by Equation (17). These data are replotted in Figure 11 and compared with Equation (25) having a pproximated by Equation (18). The limited wave slope measurements apparently favor Equation (24) or Phillips spectrum expressed in Equation (1) rather than Equation (25) or Toba spectrum expressed in Equation (5).

The fair agreement between the wave slope measurements and the prediction of the wave slope as expressed in Equation (24) may suggest that the remote sensing  $\overline{s^2}$  could lead to estimating the wind field, u, provided that the dominant wave frequency n were measured independently.

#### Prediction of Wave Spectrum

We have derived a general wave spectrum for the energy-containing range as expressed in Equation (15), in which the spectral density,  $\phi$  (n), is scaled by  $u_{*}C_{0}/n_{0}^{3}$ , the wave frequency, n by  $n_{0}$ , and the nondimensional coefficient r is related to  $n_{0}u_{*}/g$  by Equation (14). We also determined that in the equilibrium range, the non-dimensional coefficient ß expressed in the Phillips spectrum is indeed a function of  $n_{0}u_{*}/g$ . Thus, the prediction of wave spectrum becomes a task of predicting  $n_{0}u_{*}/g$ . Because of interest in predicting  $n_{0}u_{*}/g$  for fetchlimited wind waves, Lin's paper (15) is further extended for fetchlimited wind waves generated by 4 non-uniform wind flow.

At limited fetches, the effective wind wave drag,  $\tau_w$  may be approximated by

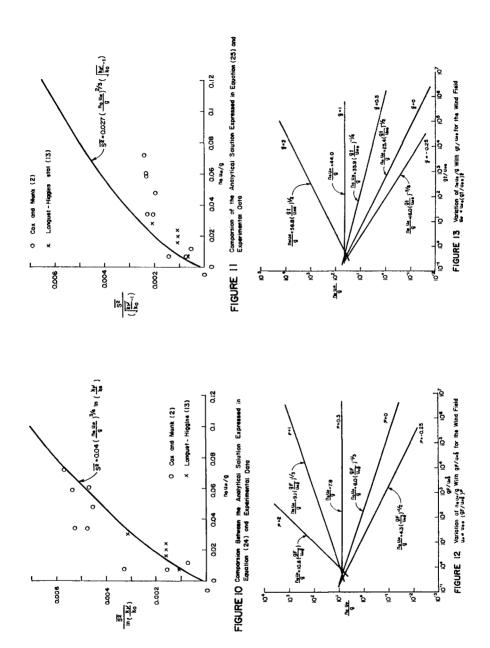
$$\tau_{w} = A_2 \rho_a u_{\star}^{2}$$
(26)

where A<sub>2</sub> is a non-dimensional numerical coefficient,  $\rho$  is the density of<sup>2</sup> the air. For a non-uniform wind flow depending on the fetch, F, or the duration, t, according to the power laws

$$u_{*} = u_{*0} \left(\frac{gF}{2}\right)^{p}$$
 (27)

$$u_{*} = u_{*0} \left(\frac{gt}{u_{*0}}\right)^{q}$$
 (28)

476



where  $u_{\star_0}$  is a reference wind speed, Equations (10) and (26) can be solved analytically and have the special solutions,

$$\frac{n_{o}u_{\star}}{g} = \left[\frac{6\rho_{a}A_{2}}{(2+5p)\rho_{w}A_{1}}\right]^{-1/3} \qquad \left(\frac{gF}{u_{\star o}^{2}}\right)^{-(1-2p)/3}$$
(29)

$$\frac{n_{o}u_{\star}}{g} = \left[\frac{\rho_{a}A_{2}}{(1+2q)\rho_{w}A_{1}}\right]^{-1/2} \left(\frac{gt}{u_{\star 0}}\right)^{-(1-q)/2}$$
(30)

for p > -2/5 and q > -1/2. When  $p \le -2/5$  or  $q \le -1/2$ , the wind wave solution is not meaningful as  $n_0 u_*/g$  becomes zero or imaginary. Figures 12 and 13 present  $n_0 u_*/g$  vs.  $gF/u_{*0}^2$  and  $gt/u_{*0}$  respectively for a family of the parameters p and q when  $A_1 = 0.044$ ,  $A_2 = 0.057$  and  $\rho_a/\rho_w = 0.0012$ .

# Conclusions and Recommendations

An empirical wave spectrum in the energy-containing range for a general sea state was derived as expressed in Equation (15). The Pierson and Moskowitz spectrum, as presented in Equation (2), is a special case of Equation (15). The scaling factor of the wave frequency spectrum is  $u_{\star}C_{0}/n_{0}^{3}$ , while the scaling factor of the wave frequency n is the dominant wave frequency n. The non-dimensional numerical coefficient r is the only free parameter in the empirical equation and it can be estimated from the slope of the rear face of spectrum and approximated by the empirical formula expressed in Equation (14) for  $n_{0}u_{\star}/g$  ranging from 0.017 to 2.1.

In the equilibrium range, the saturated wave frequency spectrum is better approximated by the Phillips spectrum expressed in Equation (1) rather than the Toba spectrum expressed in Equation (5). One must point out that the wave slope data used to test the Phillips spectrum and the Toba spectrum are available from only three sources, namely Cox (2a), Cox and Munk (2), and Longuet-Higgins, et al (13). In order to establish the statistical significance of the present conclusion, additional data are required. It is recommended to perform spectral measurements of both wave variances and wave slope simultaneously at the same physical location. The wave slope can readily be measured using remote sensing technique, while the laser displacement gauge (LDG) developed by Liu and Lin (12) may be modified to measure the wave height remotely in the field.

### Acknowledgement

This paper was prepared under an IR&D funding available from the Ocean Wave Energy Conservation Program of United Industries Corporation. References

la. Battjes, J. A., Zitman, T. J. and Holthuijsen, L. H. (1986). The JONSWAP Data Reanalyzed. <u>The 20th Intl. Conf. Coastal Engineer-</u> ing, Taipei, Taiwan, R.O.C., Nov. 9-14. Burling, R. W. (1959). The Spectrum of Wave at Short Fetches. ĩ. Dtsch. Hydrogr. Z., 12: 45-64, and 96-117. Cox, C. and Munk, W. (1954). Measurement of the Roughness of 2. the Sea Surface from Photographs of the Sun's Glitter. J. Opt. Soc. Amer., 44 (11):838-850. 2a. Cox, C. S. (1958). Measurements of Slopes of High Frequency Wind Waves. J. Mar. Res., 16: 199-225. Dobson, F. W. (1971). Measurements of Atmospheric Pressure on 3. Wind Generated Sea Waves. J. Fluid Mech., 48:91. 4. Donelan, M.A., (1978). Whitecaps and Momentum Transfer. Turbulent Fluxes through the Sea Surface, Wave Dynamics and Prediction, Favre, A. and Hasselmann, K., eds., Plenum Press, pp. 273 - 287. Donelan, M. A., Hamilton, J. and Hui, W. H. (1985). Directional 4a. Spectra of Wind-Generated Waves. Phil. Trans. R. Soc. Lond., A315: 509-562. Elliott, J.A. (1972). Microscale Pressure Fluctuation Near 5. Waves being Generated by the Wind. J. Fluid Mech., 54:427. Hasselmann, K., Barnett, T.P., et al. (1973). Measurements of 6. Wind-wave Growth and Swell Decay During the Joint North Sea Wave Project (JONSWAP). <u>Deut, Hydrogr.Z.</u>, Suppl. A <u>8</u>, No. 12. Hasselmann, K., Ross, D. B., Von Müller, P., and Sell, W. 7. (1976). A Parametric Wave Prediction Model. J. Phys. Oceano., 6:200-228. Huang, N.E., Long, S.R., Tung, C.C., Yuen, Y. and Bliven, L. F. 8. (1981). A Unified Two-Parameter Wave Spectral Model for a General Sea J. Fluid Mech., 112:203-224. State. Kitaigoroskii, S.A., Krasitskii, V.P. and Zaslavskii, M.M. 9. (1975). On Phillips' Theory of Equilibrium Range in the Spectra of Wind-generated Gravity waves. J. Phys Oceanog., 5: 410-420. 10. Kitaigorodskii, S. A., Donelan, M.A., Lumley, J.L. and Terray, E.A. (1983). Wave-Turbulence Interactions in the Upper Ocean. Part II Statistical Characteristics of Wave and Turbulent Components of the Random Velocity Field in the Marine Surface Layer. J. Phys. Oceano, 13:1988-1999. lla. Lin, J. T., Gad-el-Hak, M. and Lin, H. T. (1978). A Study to Conduct Experiments Concerning Turbulent Dispersion of Oil Slicks. Report No. CG-D-54-78 and AD-AO58802, prepared for U.S. Dept. Transportation, U.S. Coast Guard. 11. Lin, J. T. (1985). Empirical Prediction of Wind-Generated Gravity Waves. Presented at the ASCE West Coast Regional Coastal Design Conference, Oakland, Ca., Nov. 7-8. 12. Liu, H. T. and Lin, J. T. (1982). On Spectrum of High-Frequency Wind Waves. J. Fluid Mech., 123:165 - 185. 12a. Long, S. R. and Huang, N. E. (1976). On the Variation and Growth of Wave Slope Spectra in the Capillary-Gravity Range with Increasing Wind. J. Fluid Mech., 77: 209-228. 13. Longuet-Higgins, M. S., Cartwright, D.E. and Smith, N.O. (1963). Observations of the Directional Spectrum of Sea Waves Using the Motions of a Floating Buoy. Ocean Wave Spectra, Englewood Cliffs, N.J., Prentice Hall Inc., pp. 111 - 136.

Mitsuyasu, H. (1968). On the Growth of the Spectrum of Wind-14. Generated Waves (I). Reports of Research Institute for Applied Mechanics, XVI, Vol. 55, Kyushu Univ., Japan. Mitsuyasu, H., Tasai, F., Sukara, T., Mizuno, S., Ohkusu, M., 15. Honde, T., and Rikiiski, K. (1980). Observation of the Power Spectrum of Ocean Waves Using a Clover Leaf Buoy. J. Phys. Oceanogr., 10:286-296. Moskowitz, L. (1963). Estimates of the Power Spectra for Fully 16. Developed Seas for Wind Speeds of 20 to 40 knots. Tech. Report for U.S. Navy Oceanographic Office under Contract N62306-1042. 17. Von Müller, P. (1976). <u>Parameterization of One-Dimensional</u> Wind waves Spectra and their Dependence on the State of Development. Max-Planck-Institute for Meteorology, University of Hamburg, West Germany. 18. Ou, S. H. (1980). The Equilibrium Range in Frequency Spectra of the Wind Generated Gravity Waves. Proc. 4th Conference on Ocean Engineering in Republic of China, Taiwan, ROC, Sept., pp. 217 - 227. 19. Patterson, M. M. (1974). Oceanographic Data from Hurricane Camille, Shell Co. Report. Phillips, O.M. (1958). The Equlibrium Range in the Spectra of 20. Wind Generated Waves. J. Fluid Mech., 4:426-434. 21. Phillips, O. M. (1966). The Dynamics of the Upper Ocean. The University Press, Cambridge, Great Britain. 22. Pierson, W. J. ed. (1962). The Directional Spectrum of a Wind-Generated Sea as Determined from Data Obtained by the Stereo Wave Observation Project. <u>Coll. Engng, N.Y.U., Met Pap., 2</u>, No. 6. Pierson, W. J. and Maskowitz, L., (1964). A Proposed Spectral 23. form for Fully Developed Wind Seas Based on the Similarity Theory of S. A. Kitaigorodskii. J. Geophys. Res., 69: 5181 - 6190. 24. Ross, D.B., Cardone, V.J., and Conaway, J. W. (1970). Laser and Microwave Observations of Sea-Surface Conditions for Fetch-Limited 17 to 25 m/s Winds. <u>IEEE Trans Geosci. Electronics</u>, GE-8, pp. 326. 25. Ross, D.B. and Cardone, V.J. (1974). Observations of Oceanic White Caps and Their Relation to Remote Measurements of Surface Wind Speed. J. Geophys. Res., 79:444-452. Schule, J.J. Jr., Simpson, L.S. and DeLeonibus, P.S. (1971). A 26. Study of Fetch-Limited Wave Spectra with an Airborne Laser. J. Geophys. Res., 76(18):4160-4171. Taira, K. (1972). A Field Study of the Development of Wind Wave. 27. J. Oceano. Soc., Japan, 28:187-202. 28. Thorton, E.B. (1977). Rederivation of the Saturation Range in the Frequency Spectrum of Wind Generated Gravity Waves. J. Phys <u>Oceanog.</u>, 7: 137-140. 29a. Toba, Y. C. (1972). Local Balance in the Air-Sea Boundary Processes, I. On the Growth Process of Wind Waves. J. Oceano. Soc. Japan, 28: 109-121. 29. Toba, Y. (1973). Local Balance in the Air-Sea Boundary Processes, III. On the Spectrum of Wind Waves. J. Oceano. Sec. Japan, 29: 209-220. 30. Wu, J. (1969). Wind Stress and Surface Roughness at Air-Sea Interface. J. Geophys. Res., 74 :444 - 455. 31. Wu, J., (1975). Wind Induced Drift Currents. J. Fluid Mech, 68: 49-70. Zakhorov, V. E. and Filonenko, N. N. (1967). Energy Spectrum for 32. Stockastic Oscillations of the Surface of a Liquid. Soviet Phys. Dok1., 11: 881-883.